Available online at www.sciencedirect.com
ScienceDirect
Microelectronics Reliability 48 (2008) 389–394
MICROELECTRONICS RELIABILITY
www.elsevier.com/locate/microrel

Characteristics of ZnO thin films prepared by radio frequency magnetron sputtering

Ping-Feng Yang [a,b], Hua-Chiang Wen [c], Sheng-Rui Jian [d], Yi-Shao Lai [a], Sean Wu [e], Rong-Sheng Chen [b,*]

[a] Central Labs, Advanced Semiconductor Engineering, Inc., 26 Chin 3rd Road, Nantze Export Processing Zone, 811 Nantze, Kaohsiung, Taiwan
[b] Department of Engineering Science, National Cheng Kung University, No. 1, University Road, 701 Tainan, Taiwan
[c] Department of Mechanical Engineering, National Chiao Tung University, 300 Hsinchu, Taiwan
[d] Department of Materials Science and Engineering, I-Shou University, 840 Kaohsiung, Taiwan
[e] Department of Electronics Engineering and Computer Sciences, Tung-Fang Institute of Technology, 829 Kaohsiung, Taiwan

Received 15 January 2007; received in revised form 31 August 2007
Available online 22 October 2007

Abstract

We investigated in this study structural and nanomechanical properties of zinc oxide (ZnO) thin films deposited onto Langasite substrates at 200 °C through radio frequency magnetron sputtering with an radio frequency power at 200 W in an O_2/Ar gas mixture for different deposition time at 1, 2, and 3 h. Surface morphologies and crystalline structural characteristics were examined using X-ray diffraction, scanning electron microscopy, and atomic force microscopy. The deposited film featured a polycrystalline nature, with (100), (002), and (101) peaks of hexagonal zinc oxide at 31.75°, 34.35°, and 36.31°. As the deposition time increased, the ZnO film became predominantly oriented along the *c*-axis (002) and the surface roughness decreased. Through Berkovich nanoindentation following a continuous stiffness measurement technique, the hardness and Young's modulus of ZnO thin films increased as the deposition time increased, with the best results being obtained for the deposition time of 3 h. In addition, surface acoustic wave properties of ZnO thin films were also presented.

1. Introduction

The ZnO thin film, one of the II–VI compound semiconductors, is composed of hexagonal wurtzite crystal structure ($a = 3.249$ Å, $c = 5.2057$ Å). Owing to its high optical transmittance in the visible light region, the ZnO thin film finds its applications mainly as a transparent conductive film as well as the solar cell window. The ZnO is also a promising piezoelectric material because of its high coupling factor and its simple composition [1].

The ZnO thin film can be deposited by various methods such as spray pyrolysis [2–4], chemical vapor deposition (CVD) [5,6], sol–gel process [7–9], sputtering techniques [10–12], chemical spray [13], plasma enhanced CVD [14], and pulsed laser deposition (PLD) [15]. Among these methods, reactive radio frequency (r.f.) magnetron sputtering shows great advantages: it only requires a very simple apparatus, has a high deposition rate, and is capable of depositing on a large area.

Microelectromechanical systems (MEMS) serve as sensors or actuators, for which piezoelectricity usually plays a consequential role in sensing or generating forces and torques. Langasite ($La_3Ga_5SiO_{14}$, LGS) monocrystal is an attractive piezoelectric substrate for implementing IF band small size and wide band surface acoustic wave (SAW) filters because of its larger piezoelectric coupling constant, slower velocity than those of quartz and good temperature stability [16–18]. LGS was shown to have piezoelectrically induced bulk acoustic waves under a temperature up to at least 1050 °C [19] and does not undergo any phase

* Corresponding author. Tel.: +886 6 275 7575x63328; fax: +886 6 276 6549.
E-mail address: rschen@mail.ncku.edu.tw (R.-S. Chen).

0026-2714/$ - see front matter © 2007 Elsevier Ltd. All rights reserved.
doi:10.1016/j.microrel.2007.08.010

transition up to its melting temperature at 1473 °C [20,21]. The crystal quality and characterization of the material with appropriate crystal constants were focused on in early work [22,23]. Langasite-type crystals show excellent piezoelectric properties led by their large electromechanical coupling factors.

In this study, we focused on structural, mechanical, and electromechanical coupling properties of highly *c*-axis-oriented ZnO thin films deposited onto Langasite substrates through r.f. magnetron sputtering by means of X-ray diffraction (XRD), atomic force microscopy (AFM), nanoindentation techniques, and surface acoustic wave (SAW) measurements. The influence of various deposition time of ZnO thin films was also presented.

2. Experiment descriptions

The ZnO thin films were deposited onto Langasite substrates by magnetron sputtering so that double-layered ZnO/Langasite composites were produced. A zinc disc was used as the target (purity at 99.999 at.%). The r.f. power, ambient pressure of oxygen and argon gases (O_2/($Ar + O_2$) ratio 20%), and substrate temperature were set at 200 W, 0.8 mPa, and 200 °C, respectively. The deposition time was 1, 2, or 3 h. Crystalline structure and crystallographic orientation of ZnO thin films were determined using grazing incident angle XRD (PANalytical X'Pert PRO). The power of XRD (Cu Kα radiation) was fixed at 45 kV and 40 mA. The incident angle of X-ray was fixed at 0.5°. In order to compare the (0 0 2) diffraction intensities of different sputtering samples, the XRD diffraction angles (2θ) spanned from 30° to 60°. The thickness and morphology of the ZnO layer (ZnO) was determined by scanning electron microscopy (Hitachi 4700). Atomic force microscopy (Veeco Dimension 5000 Scanning Probe Microscope) was employed to characterize microstructures of the coatings.

Successful implementation of thin films concerns greatly with their mechanical properties. Mechanical characterizations of materials, however, are scale-dependent, and as a result, a thin film may feature mechanical properties different from a bulk material. For thin films, nanoindentation is often used to characterize their hardness and Young's moduli [24–27]. In this study, mechanical properties of r.f. magnetron sputtered ZnO thin films were characterized by Nano Indenter XP systems (MTS Cooperation, Nano Instruments Innovation Center, Oak Ridge, TN, USA) using a diamond Berkovich indenter tip (tip radius ~50 nm), which is preferred for low-load indentation testing. Albeit all real indenters are rounded at some small scale, tip rounding on Berkovich pyramids is usually limited to 100 nm, and therefore plasticity initiates at very small loads. Because the Berkovich pyramid induces nominally the same strain as the conventional Vickers pyramid does, hardness data taken with a Berkovich pyramid (HB) may be directly converted to the Vickers hardness (VHN) [28,29]. The continuous contact stiffness measurement (CSM) was incorporated in nanoindentation, which was accomplished by superimposing small oscillations at 75 Hz on the force signal to measure displacement responses. The CSM technique helps acquire hardness and Young's modulus with respect to the indentation depth during indentation [30,31]. The indenter was loaded and unload three times to ensure that the tip was in proper contact with the surface of the specimen. The indenter was then loaded with a strain rate of 0.05 s^{-1} and held at the peak load for 60 s before unloading. The method proposed by Oliver and Pharr [30] was used to extract hardness and Young's modulus of the specimen from the load–displacement curve. The Poisson's ratio was set as 0.25. The Young's modulus corresponds to an isotropic approximation related to a specific combination of independent elastic constants of the ZnO thin film along the indentation direction.

3. Results and discussion

3.1. Crystalline structure and surface morphology (XRD, SEM, AFM)

Fig. 1 features X-ray diffraction spectra of ZnO thin films deposited with different deposition time. For 1 h deposition, weak diffraction peaks of ZnO were observed, referring to the beginning stage of ZnO growth. The spectrum for 2 h deposition indicates the presence of pure and polycrystalline ZnO in a wurtzite structure [32]. Intensities of the spectrum peaks magnified significantly as the deposition time increased to 3 h, and that indicates an improvement of the crystalline quality with time.

The deposited film featured a polycrystalline nature, with (1 0 0), (0 0 2), and (1 0 1) peaks of hexagonal ZnO at 31.75°, 34.35°, and 36.31°. Previous work [33,34] showed that the films deposited by dc magnetron sputtering at a substrate temperature of 50 °C had a preferred orientation along the (0 0 2) plane, a random orientation at 200–300 °C,

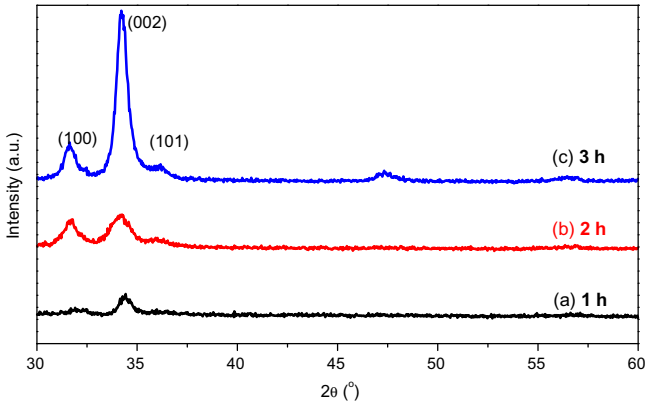

Fig. 1. XRD spectra of ZnO thin films deposited with different deposition time: (a) 1 h – weak diffraction peaks of ZnO, (b) 2 h – presence of pure and polycrystalline ZnO, and (c) 3 h – improvement of crystalline quality with time.

and again a preferred orientation along the (002) crystal plane at 350–480 °C. For r.f. magnetron sputtering as in this case, the deposited films were found to feature mixed orientations at a substrate temperature of 200 °C. Moreover, as the deposition time increased, the *c*-axis (002) peak was sharply magnified while the other two peaks coexisted but with much smaller intensities and greater FWHM (full width at half maximum). We note that the grain size of a film can be estimated using Scherrer's equation [35], $D = 0.9\lambda/\beta\cos\theta$, where D is the mean dimension of the crystallites, λ the X-ray wavelength, and β the FWHM of the (002) peak. From the XRD analysis, the grain size of the film decreased from 208, 187, to 140 nm with the increase of the deposition time from 1, 2, to 3 h, indicating that the crystallinity along the *c*-axis improved as the deposition time increased. Deposition up to 1 h probably only disturbed the oriented crystal growth because of the random atomic arrangement of the substrate, while the nucleation of ZnO apparently occurred on the substrate interface from 2 to 3 h because the peak intensity of the (002) plane was observed. The oriented grain growth may be readily triggered due to the presence of slightly oriented grains, and hence the peak intensity of the (002) plane increased abruptly as the deposition time increased.

Fig. 2 shows SEM images and AFM inspections, respectively, of surface morphologies of ZnO thin films deposited with different deposition time. It is suggested that the Langasite substrate surface do not have a specific epitaxial orientation to follow, which results in randomly oriented nuclei. Therefore, the RMS (root mean square) surface roughness of ZnO thin films decreased from 20.6, 18.5, to 13.5 nm as the deposition time increased from 1, 2, to 3 h. Clearly, as the deposition time increased, surface morphologies of the films became smooth and grains grew and distributed uniformly.

Fig. 3 shows cross-sectional SEM images of ZnO thin films deposited with different deposition time. The thickness of ZnO thin films increased regularly from 1.5, 3, to 4.5 nm as the deposition time increased from 1, 2,

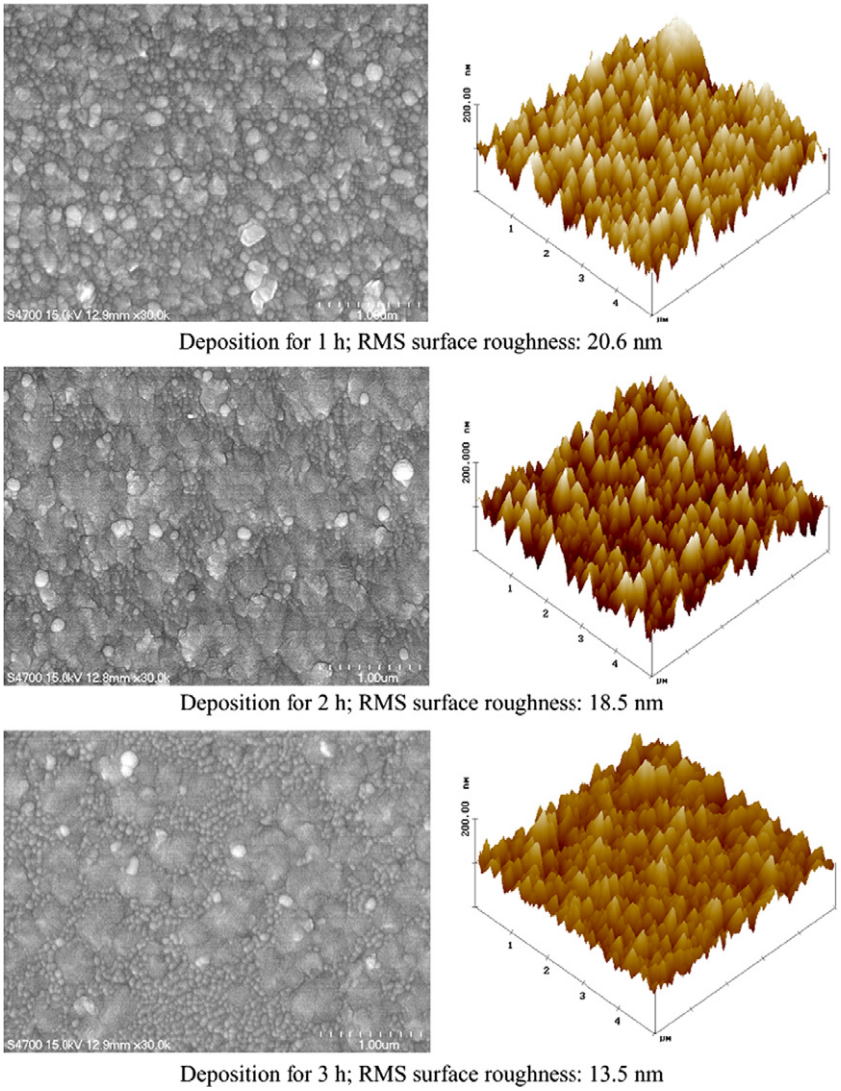

Fig. 2. SEM and AFM images of surface morphologies of ZnO thin films with different deposition time.

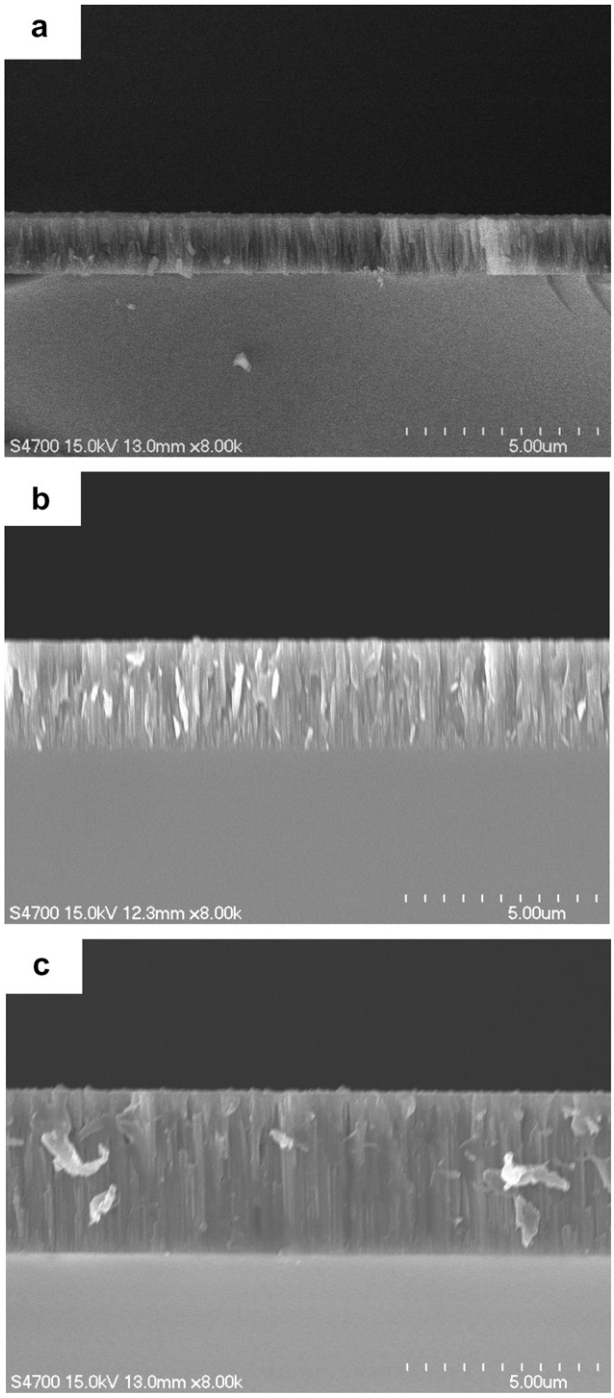

Fig. 3. Cross-sectional images of ZnO thin films deposited for (a) 1 h, (b) 2 h, and (c) 3 h.

to 3 h, respectively. Columnar structures were observed in the ZnO thin films, whose possible formation stages have been proposed [36,37]. Note that distinct columnar structures and even voiding defects inside the ZnO thin film may be encountered using a different sputtering method [38]. Our experiments clearly demonstrated that the crystalline structure of ZnO thin film can be deposited reliably through r.f. magnetron sputtering with regular parameter controls.

3.2. Nanoindentation characterizations

Figs. 4 and 5 show hardness and Young's moduli, respectively, of ZnO thin films deposited with different deposition time as functions of the indentation depth, following the method proposed by Oliver and Pharr [30]. For indentation depths up to about 10 nm, the hardness increased as the indentation depth increased, which is usually attributed to the transition between purely elastic to elastoplastic contact whereby the hardness is actually the contact pressure. For indentation depths greater than about 10 nm, the hardness of ZnO thin films became constant. Young's modulus followed a trend similar to that of the hardness except that its magnitude converged at an indentation depth smaller than that for hardness. Hardness and Young's moduli were therefore determined by averaging measurements at indentation depths from 100 to 200 nm, considering an adequate depth to achieve a fully

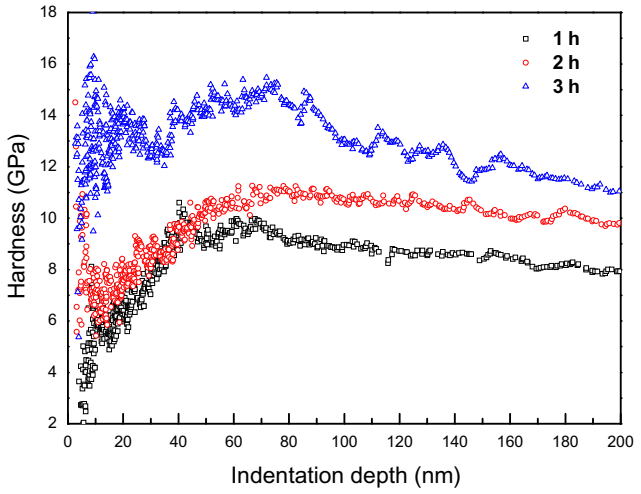

Fig. 4. Hardness of ZnO thin films with different deposition time as functions of indentation depth.

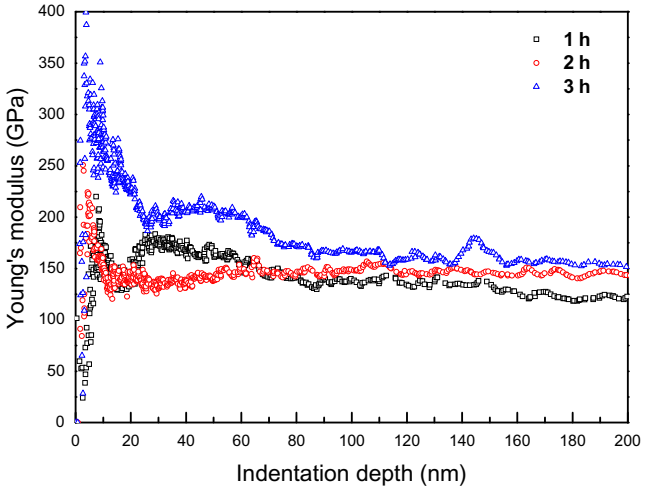

Fig. 5. Young's moduli of ZnO thin films with different deposition time as functions of indentation depth.

Table 1
Mechanical properties of ZnO thin films obtained by nanoindentation

Sample	Hardness (GPa)	Young's modulus (GPa)
ZnO/Langasite (1 h)[a]	9.2 ± 0.8	135.4 ± 6.4
ZnO/Langasite (2 h)[a]	9.4 ± 2.8	147.3 ± 4.5
ZnO/Langasite (3 h)[a]	10.4 ± 0.4	157.9 ± 2.8
ZnO/*c*-sapphire[b]	5.8 ± 0.8	310 ± 40
ZnO bulk (*a*-axis)[b]	4.8 ± 0.2	143 ± 6
ZnO/*a*-sapphire[b]	6.6 ± 1.2	318 ± 50
ZnO bulk (*c*-axis)[b]	2.0 ± 0.2	163 ± 6

[a] Present study.
[b] Coleman et al. [39].

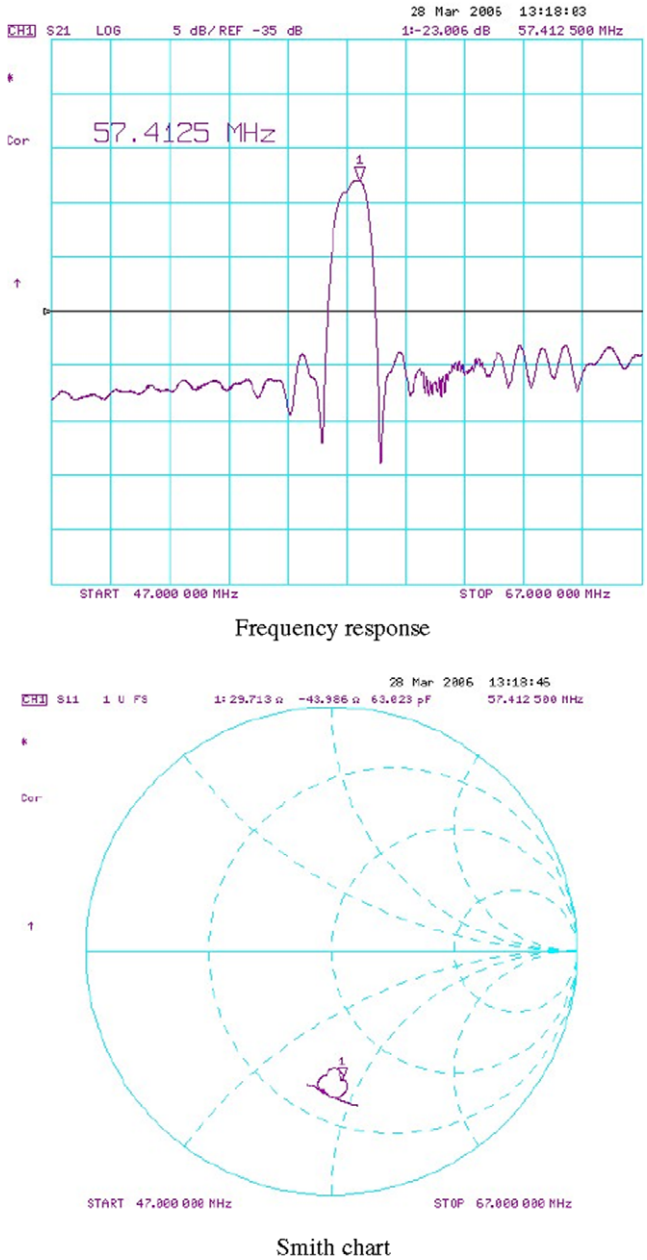

Fig. 6. Frequency response (s21) and smith chart (s11) of Langasite coated with 1.76 μm thick ZnO thin film.

developed plastic zone and meanwhile not exceeding 20% of the film thickness to avoid the substrate effect [14]. For deposition time at 1, 2, and 3 h, hardness of ZnO thin films was 9.2 ± 0.8, 9.4 ± 2.8, and 10.4 ± 0.4 GPa, respectively, while Young's moduli were 135.4 ± 6.4, 147.3 ± 4.5, and 157.9 ± 2.8 GPa, respectively.

Comparisons of hardness and Young's moduli of ZnO thin films with the magnitudes reported by Coleman et al. [39] are shown in Table 1. Unlike the monocrystalline structure focused on by Coleman et al. [39], in our experiments, polycrystalline ZnO in a wurtzite structure was present, whose *c*-axis crystalline quality improved with increasing deposition time. Well nucleated ZnO occurred on the substrate interface from 2 to 3 h and this accompanied with the enhancement in its mechanical resistance against elastic and elastoplastic deformations.

3.3. SAW measurement

Fig. 6 shows frequency response of s21 and smith chart of s11 of Langasite coated with a 1.76 μm thick ZnO thin film. The center frequency was 57.41 MHz and the SAW velocity calculated was 2756 m/s. The impedance at the center frequency was $29.713 + j(-43.986)\ \Omega$ and the electromechanical coupling coefficient (K^2) calculated from the data was 1.18%. For the original Langasite substrate, K^2 was 0.38% and the SAW velocity was 2732 m/s. Clearly, coating of a ZnO thin film on Langasite slightly enhances the SAW velocity while effectively enhances electromechanical coupling.

4. Conclusion

The XRD, SEM, AFM, and nanoindentation techniques have been used to investigate surface features and nanomechanical properties of ZnO thin films deposited onto Langasite substrates through r.f. magnetron sputtering with different deposition time. The XRD analysis showed that the deposited film featured a polycrystalline nature, with (100), (002), and (101) peaks of hexagonal ZnO at 31.75°, 34.35°, and 36.31°. As the deposition time increased, the ZnO thin film became predominantly oriented along the *c*-axis (002) and the surface roughness decreased. Results from Berkovich nanoindentation indicated that the hardness of ZnO thin films deposited for 1–3 h ranged from 9.2 ± 0.8 to 10.4 ± 0.4 GPa while the Young's modulus ranged from 135.4 ± 6.4 to 157.9 ± 2.8 GPa. Through SAW measurements, coating of ZnO thin films was shown to effectively enhance electromechanical coupling of Langasite.

Acknowledgement

This work was partially supported by National Science Council of Taiwan through Grant NSC 96-2112-M-009-017.

References

[1] Yoon KH, Choi J-W, Lee D-H. Characteristics of ZnO thin films deposited onto Al/Si substrates by r.f. magnetron sputtering. Thin Solid Films 1997;302:116–21.

[2] Studenikin SA, Golego N, Cocivera M. Fabrication of green and orange photoluminescent, undoped ZnO films using spray pyrolysis. J Appl Phys 1998;84(4):2287–94.

[3] Paraguay DF, Estrada LW, Acosta NDR, Andrade E, Miki-Yoshida M. Growth, structure and optical characterization of high quality ZnO thin films obtained by spray pyrolysis. Thin Solid Films 1999;350:192–202.

[4] Bender M, Gagaoudakis E, Douloufakis E, Natsakou E, Katsarakis N, Cimalla V, et al. Production and characterization of zinc oxide thin films for room temperature ozone sensing. Thin Solid Films 2002;418:45–50.

[5] Takikawa H, Kimura K, Miyano R, Sakakibara T. ZnO film formation using a steered and shielded reactive vacuum arc deposition. Thin Solid Films 2000;377–378:74–80.

[6] Roy S, Basu S. Improved zinc oxide film for gas sensor applications. Bull Mater Sci 2002;25(6):513–5.

[7] Bao D, Gu H, Kuang A. Sol–gel-derived *c*-axis oriented ZnO thin films. Thin Solid Films 1998;312:37–9.

[8] Ryu H-W, Park B-S, Akbar SA, Lee W-S, Hong K-J, Seo Y-J, et al. ZnO sol–gel derived porous film for CO gas sensing. Sen Actuators, B: Chem 2003;96(3):717–22.

[9] Kamalasanan MN, Chandra S. Sol–gel synthesis of ZnO thin films. Thin Solid Films 1996;288:112–5.

[10] Water W, Chu S-Y. Physical and structural properties of ZnO sputtered films. Mater Lett 2002;55:67–72.

[11] Lu YM, Hwang WS, Liu WY, Yang JS. Effect of RF power on optical and electrical properties of ZnO thin film by magnetron sputtering. Mater Chem Phys 2001;72(2):269–72.

[12] Nunes P, Costa D, Fortunato E, Martins R. Performances presented by zinc oxide thin films deposited by r.f. magnetron sputtering. Vacuum 2002;64(3–4):293–7.

[13] Olvera M de la L, Maldonado A, Asomoza R, Tirado-Guerra S. Characteristics of transparent and conductive undoped ZnO thin films obtained by chemical spray using zinc pentanedionate. Thin Solid Films 2002;411:198–202.

[14] Li BS, Liu YC, Shen DZ, Zhang JY, Lu YM, Fan XW. Effects of RF power on properties of ZnO thin films grown on Si (0 0 1) substrate by plasma enhanced chemical vapor deposition. J Cryst Growth 2003;249:179–85.

[15] Kotlyarchuk B, Savchuk V, Oszwaldowski M. Preparation of undoped and indium doped ZnO thin films by pulsed laser deposition method. Cryst Res Technol 2005;40(12):1118–23.

[16] Gualtieri JG, Kosinski JA, Ballato A. Piezoelectric materials for acoustic wave applications. IEEE Trans Ultrason Ferroelect Freq Control 1994;41(1):53–9.

[17] Sakharov S, Senushencov P, Medvedev A, Pisarevsky Yu. New data on temperature stability and acoustical losses of langasite crystals. In: Proceedings of 49th IEEE international frequency control symposium, San Francisco, CA, USA; 1995. p. 647–52.

[18] Satoh H, Mori A. Surface acoustics wave propagation characteristics on a langasite crystal plate. Japanese J Appl Phys 1997;36:3071–3.

[19] Fritze H, Schulz M, Seh H, Tuller HL. High temperature operation and stability of langasite resonators. MRS Symp Proc 2005;828:145–50.

[20] Shimamura K, Takeda H, Kohno T, Fukuda T. Growth and characterization of lanthanum gallium silicate $La_3Ga_5SiO_{14}$ single crystals for piezoelectric applications. J Cryst Growth 1996;163(4):388–92.

[21] Chai B, Lefaucheur JL, Ji YY, Qui H. Growth and evaluation of large size LGS ($La_3Ga_5SiO_{14}$) LGN ($La_3Ga_{5.5}Nb_{0.5}O_{14}$) and LGT ($La_3Ga_{5.5}Ta_{0.5}O_{14}$) single crystals. In: Proceedings of 1998 IEEE international frequency control symposium, Pasadena, CA, USA; 1998. p. 748–60.

[22] Kaminskii AA, Silvestrova IM, Sarkisov SE, Denisenko GA. Investigation of trigonal $(La_{-1-x}Nd_x)_3Ga_5SiO_{14}$ crystals. II. Spectral laser and electromechanical properties. Phys Status Solidi A 1983;80(2):607–20.

[23] Silverstrova IM, Bezdelkin VV, Senyushenkov PA, Pisarevsky YV. Present stage of $La_3Ga_5SiO_{14}$-research. In: Proceedings of 1993 IEEE international frequency control symposium, Salt Lake City, UT, USA; 1993. p. 348–50.

[24] Jian S-R, Fang T-H, Chuu D-S. Nanoindentation investigation of amorphous hydrogenated carbon thin films deposited by ECR-MPCVD. J Non-Cryst Solids 2004;333(3):291–5.

[25] Beake BD, Lau SP. Nanotribological and nanomechanical properties of 5–80 nm tetrahedral amorphous carbon films on silicon. Diamond Relat Mater 2005;14(9):1535–42.

[26] Martyniuk M, Sewell RH, Musca CA, Dell JM, Faraone L. Nanoindentation of HgCdTe prepared by molecular beam epitaxy. Appl Phys Lett 2005;87(25):251905-1–5-3.

[27] Jian S-R, Fang T-H, Chuu D-S. Nanomechanical characterizations of InGaN thin films. Appl Surf Sci 2006;252(8):3033–42.

[28] Kim J-Y, Read DT, Kwon D. Depth-dependent hardness characterization by nanoindentation using a Berkovich indenter with a rounded tip. MRS Proc 2005;875(6):02.4.1–6.

[29] Gong J, Miao H, Peng Z. Analysis of the nanoindentation data measured with a Berkovich indenter for brittle materials: effect of the residual contact stress. Acta Mater 2004;52(3):785–93.

[30] Oliver WC, Pharr GM. An improved technique for determining hardness and elastic modulus using load and displacement sensing indentation experiments. J Mater Res 1992;7(6):1564–83.

[31] Hay JL, Pharr GM. Instrumented indentation testing. In: Kuhn H, Medlin D, editors. ASM handbook. Material testing and evaluation, vol. 8. Materials Park, OH, USA: ASM International; 2000. p. 232–43.

[32] Schulz H, Thiemann KH. Structure parameters and polarity of the wurtzite type compounds Sic-2H and ZnO. Solid State Commun 1979;32(9):783–5.

[33] Kim YJ, Kim YT, Yang HK, Park JC, Han JI, Lee YE, et al. Epitaxial growth of ZnO thin films on R-plane sapphire substrate by radio frequency magnetron sputtering. J Vacuum Sci Technol A 1997;15(3):1103–7.

[34] Meng L-J, Andritschky M, dos Santos MP. Zinc oxide films prepared by dc reactive magnetron sputtering at different substrate temperatures. Vacuum 1994;45(1):19–22.

[35] Lim WT, Lee CH. Highly oriented ZnO thin films deposited on Ru/Si substrates. Thin Solid Films 1999;353:12–5.

[36] Shin JW, Lee JY, Kim TW, No YS, Cho WJ, Choi WK. Growth mechanisms of thin-film columnar structures in zinc oxide on p-type silicon substrates. Appl Phys Lett 2006;88:091911.

[37] Yuk JM, Lee JY, Jung JH, Kim TW, Son DI, Choi WK. Initial formation mechanisms of the supersaturation region and the columnar structure in ZnO thin films grown on n-Si(0 0 1) substrates. Appl Phys Lett 2007;90:031907.

[38] Gao W, Li Z. ZnO thin films produced by magnetron sputtering. Ceram Int 2004;30(7):1155–9.

[39] Coleman VA, Bradby JE, Jagadish C, Munroe P, Heo YW, Pearton SJ, et al. Mechanical properties of ZnO epitaxial layers grown on *a*- and *c*-axis sapphire. Appl Phys Lett 2005;86:203105.